THE EFFECT OF SINTERING TEMPERATURE ON THE STRUCTURE AND DEGRADABILITY OF STRONTIUM-DOPED CALCIUM POLYPHOSPHATE BIOCERAMICS

QIANBIN WANG, QIGUANG WANG, XIAOHUA ZHANG, XIXUN YU, CHANGXIU WAN

College of Polymer Materials and Engineering, Sichuan University, Cheng du 610065, P. R. China

E-mail: wanchangxiu@163.com

Submitted November 11, 2010; accepted April 7, 2010

Keywords: Strontium-doped calcium polyphosphate, Sintering temperature, Structure, Degradability

Calcium polyphosphate-based bioceramic composites containing 1 mol% Sr^{2+}, assigned as strontium-doped calcium polyphosphate (SCPP), were prepared. Effect of sintering temperature (700, 800 and 900°C) on the microstructure and degradability of SCPP bioceramic were investigated. The result indicated that the strontium doped did not affect the crystal system and space group of calcium polyphosphate. The crystal structure of SCPP samples sintered at 700, 800 and 900°C was identified as β-CPP. The density and grain size of prepared samples increased with the increase of sintering temperature, from 2.46 g/cm3 and 2.33 μm at 700°C to 2.60 g/cm^3 and 4.46 μm at 900°C. The in vitro degradation behavior of SCPP indicated the increase of the degradation rate with the sintering temperature.

INTRODUCTION

Biodegradable calcium polyphosphate ceramics (CPP), a kind of inorganic polymeric biomaterials, has drawn attention due to its controllable degradability [1-3], outstanding biocompatibility [3-5], excellent mechanical property, similar chemical elements with bones and diversity in chemical composition [6, 7]. Piliar, et al. [8-11] studying the structure (the theoretical density of CPP is 2.89g/cm^3), mechanical strength and in vitro degradability of porous CPP samples, suggested its potential as a bone substitute. The research of Lee [12] demonstrated the possibility of using a porous CPP matrix as biodegradable scaffold in vitro along with attached marrow-derived mesenchymal cells for transplantation for bone regeneration in vivo. Previous studies by Qiu et al. [13] exploring the effect of the polymerization degree on the mechanical performance and degradation rate of CPP showed that with the increase of the polymerization degree, the compressive strength was promoted and the degradability was weaken. And all of these studies indicated that CPP was an ideal bioceramics with excellent osteoinduction and osteoconduction for bone substitute.

In order to optimize the degradability of CPP and promoting its biological function, strontium ion was doped into CPP. Strontium, a kind of osteoinductive trace elements [14], was incorporated into CPP crystalline structure, assigning as strontium-doped calcium polyphosphate (SCPP). In recent years, strontium has been gradually recognized during the research of treatment for osteoporosis. It enhances the proliferation of osteoblastic cells, and simulates bone formation in calvarial cultures in vitro [15]. Furthermore, a few articles demonstrated that strontium ranelate decreased bone resorption in vitro [16, 17]. The result of increase in bone mineral density seems to be associated with enhanced mechanical property. Moreover, strontium has various effects on bone metabolism depending on the dosage. Previous studies by Qiu et al. [18] explored that the porous SCPP which contained 1 % strontium was optimal according to the result of MTT and ALP activity assay. After investigating the biocompatibility and osteogenesis as well as degradability of the porous strontium-doped calcium polyphosphate (SCPP) scaffolds in vivo, Tian [19] demonstrated that SCPP scaffold can be considered as a biocompatible material, making it attractive for bone substitute application purposes. The feasibility of these researches showed that the porous SCPP may be a new promising biomaterial for bone tissue engineering.

The aim of the present work was to study the effect of sintering temperature on the structure and degradability of strontium-doped calcium polyphosphate. The bulk density of the samples was investigated by using Archimedes' method. And the grain size of the sample was assessed in terms of SEM pattern. In addition, the effects of sintering temperature on the immersion behaviour of sintered SCPP was also investigated.

EXPERIMENTAL

Preparation of scaffolds

SCPP samples were prepared using the following analytical chemicals: $CaCO_3$, $SrCO_3$ and H_3PO_4 (85 %). Detailed method was described elsewhere [18]. Briefly, according to the stoichiometric use, 1% strontium-doped calcium phosphate monobasic monohydrate powders were calcined at 500ºC under atmospheric conditions, and held for 10 hours. Then these powders were calcined at 1200ºC to yield amorphous melt frit. The melted frit was promptly quenched into distilled water to avoid crystallization during cooling. The amorphous frits were milled and screened to powders in a size range of 48~75 μm.

Porous scaffolds were fabricated by mixing the stearic acid as porous agent within the amorphous powders. Cylindrical-like scaffolds were fabricated in a mold by loading 1 MPa compressive strength for 3 min. After drying, these samples were sintered at 700°C (SCPP700), 800°C (SCPP800) and 900°C (SCPP900) for 3 hours, and then cooled naturally to room temperature in a furnace to enhance the crystallization process.

Analysis of crystal structure

X-ray diffraction (XRD) analysis was used to identify the crystalline phases of SCPP. The sample was analyzed by X-ray diffraction (XRD) using a X'Pert Pro MPD X-ray diffractometer (Philips, Netherlands) with a CuKa radiation source (40 kV, 40 mA). Continuous scanning mode with 0.02 step size and 0.5 s of set time were used in all XRD experiments for collecting the data.

Thermal analysis

Differential thermal analysis (DTA) was used to determine the glass transformation temperature (T_g), crystallization temperature (T_c) and melting temperature (T_m) of the SCPP glass. The analyses were carried out in a TA-2910 (USA) using an inert nitrogen atmosphere, a heating rate of 10°C/min and a temperature scanning up to 1200°C. Al_2O_3 was used as a reference material.

Relative density and microstructure

The bulk density of the sintered SCPP samples was measured by the Archimedes immersion method. The density of the specimens was determined with the following relation:

$$\rho = \frac{W_a}{W_a - W_b}\rho_b \qquad (1)$$

where W_a and W_b are the weights of the specimen in the air and water, respectively. ρ_b is the density of water.

Microstructure analysis was carried out on a JSM-5900LV SEM operated at 20 kV. The sintered samples were prepared for SEM by polishing and applying a gold-coating. Linear-intercept technique was used to determine the grain size of composites by counting a minimum of 50 grains.

The degradation behavior of in TRIS solution

The degradation testing was performed according to ISO 10993-14 - 'Biological evaluation of medical devices - Part 14: Identification and quantification of degradation products from ceramics'. For degradation testing, each scaffold was placed in tris buffer solution (pH = 7.4) at 37 ± 0.5ºC and with a continual agitation speed of 120 rpm. At the end of each immersion time (0, 0.5, 1, 3, 5, 8, 11, 14, 17, 21, 24, 28 days), distilled water was used to wash the sample surface and samples were dried until a constant weight at 80°C was reached. The upper limpid solution of degraded solution was stored in a refrigerator for future tests.

A relative weight loss percentage of samples was calculated from the following equation:

$$Weightloss\ (\%) = \frac{W_0 - W_t}{W_0}.100 \qquad (2)$$

where W_0 and W_t stand for initial weight and weight after a specific immersion time, respectively.

The concentration of phosphorus concentration was measured from total phosphate groups by ultraviolet spectroscopy using the ammonium molybdate ultraviolet-visible spectrophotometry (AMUVS) methods [20].

RESULTS AND DISCUSSION

Effect of sintering temperature on the crystal Structure of SCPP Sample

Figure 1 showing the XRD patterns of SCPP samples sintered at different temperatures indicates almost identical crystal structure, which is not affected by the sintering temperature. There are only small differences in peak width and absolute intensity of the diffraction patterns. The comparison with the standard PDF card 77-1953 (XRD peaks of the pure β-CPP fitted by Jade 5.0) shows high similarity of characteristic peaks in each pattern, especially of three characteristic peaks between 20~30°: This fact indicates the crystal system of prepared SCPP samples corresponds to that of the β-CPP.

The crystal lattice parameters presented in Table 1 were calculated from the results of curve fitting. The result showed the cell volumes of SCPP expanded after Sr^{2+} substituting the site of Ca^{2+}. With the increase of sintering temperature, the cell volumes of SCPP decreased.

Table 1. The Lattice Parameters of SCPP with different sintering temperatures.

Sample	a (Å)	b (Å)	c (Å)	V (Å^3)
PDF 77-1953	6.999	7.717	16.944	915.14
SCPP700	7.003	7.711	16.995	918.02
SCPP800	7.009	7.705	16.983	917.06
SCPP900	7.010	7.700	16.972	916.14

Strontium and calcium are in the same group on the periodic table and have similar properties. Their atomic radii are 0.113 nm and 0.099 nm [21], respectively; their electronegativities are both 1.0. In addition, the most common valences of both elements is +2. According to the Hume-Rothery Rules [22], the strontium-doped calcium polyphosphate should have lower solubility in water. The incoming strontium ions are distributed in CPP crystal lattices without breaking the crystal structure and thus maintain the integrity of a single crystal phase. As shown in Figure 1, the crystal structure was not changed after strontium ion doping.

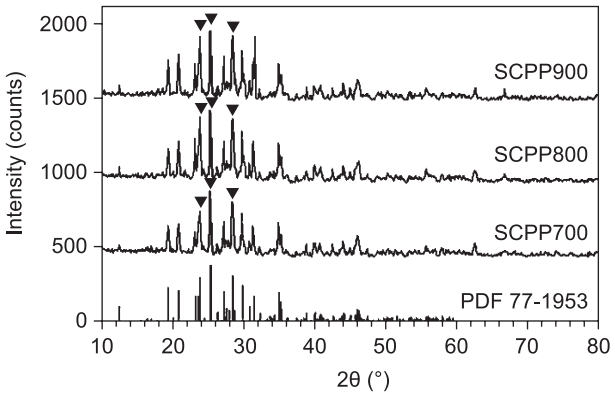

Figure 1. XRD patterns of SCPP samples sintered at temperatures 700°C, 800°C and 900°C.

DTA

A typical DTA curve of SCPP glass obtained at a heating rate of 10°C/min is shown in Figure 2. Two exothermic peaks can be observed due to crystallisation phenomena at temperatures of 634°C and 968°C, and two endothermic peaks at temperatures of 600°C and 909°C.

As the CPP is an inorganic polymer sensitive to the sintering temperature, its crystalline phases may be transformed even in a narrow temperature zone. Literatures reported [2, 13] that CPP sintered at different temperatures exhibits crystalline structures assigned as α CPP, β-CPP and γ-CPP. However, the reports of the structure characterization and crystal transformation during sintering process are ambiguous [8, 23-28]. Wang [25] showed that the diffraction spectrum of CPP sintered from 25°C to 580°C corresponds with the amorphous structure of CPP. Guo et al. [26] reported that the transformation of amorphous CPP to crystalline γ CPP occurred at 585–600°C. Some studies [27, 28] reported that the transformation of γ CPP to β-CPP occurred at 690-720°C, and the CPP sintering 900-960°C was α-CPP.

Throughout the sintering process, amorphous CPP is firstly transformed to γ CPP, then γ-CPP is transformed to β-CPP and finally β-CPP is transferred α-CPP as the following scheme indicates:

$$\begin{aligned} Ca(PO_3)_2 &\xrightarrow{25\sim580^\circ C} \text{amorphous} - Ca(PO_3)_2\,^{[24]} \\ &\xrightarrow{585\sim600^\circ C} \gamma - Ca(PO_3)_2\,^{[26]} \\ &\xrightarrow{600\sim700^\circ C} \beta - Ca(PO_3)_2\,^{[26]} \\ &\xrightarrow{900\sim960^\circ C} \alpha - Ca(PO_3)_2\,^{[28]} \end{aligned} \quad (3)$$

Figure 2 shows that SCPP samples sintered at 700 and 900°C have crystalline structures. When compared with the X-ray diffraction patterns presented in Figure 1, the crystalline structure corresponds with the β-CPP, which is a stable phase at room temperature [8, 24]. Therefore, the sintering property of CPP is not changed after strontium ion doping.

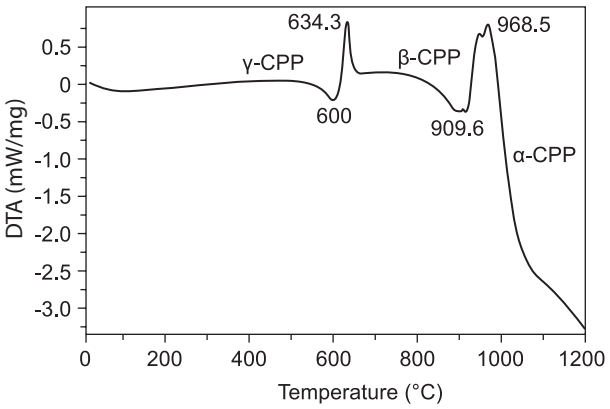

Figure 2. DTA curve of SCPP sample.

Grain size and relative density

Figure 3 presents the original surfaces of SCPP. Scaffolds synthesized at different sintering temperatures show variation in the surface morphologies.

The relative densities and grain size were affected by the sintering temperatures, as shown in Figure 4. The density and grain size of SCPP prepared at 700°C was 2.46 g/cm^3 and 2.33 μm, respectively. For specimens prepared with the same holding time (3 hours), the density increased from 2.46 g/cm^3 to 2.60 g/cm^3, when sintering temperature increased from 700 °C to 900°C. The grain size increased from 2.33 μm to 4.46 μm over the same temperature range.

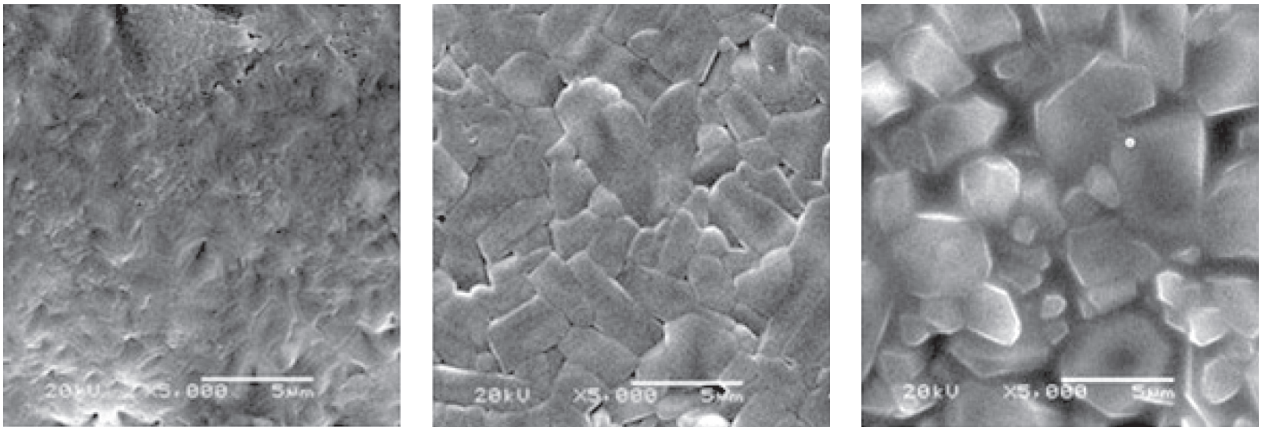

a) b) c)

Figure 3. SEM pictures of SCPP: a) SCPP700, b) SCPP800, c) SCPP900.

The increase in density was due to decrease in the porosity of the sample and enhanced the grain size. However, higher sintering temperature would cause abnormal grain growth resulted in a decrease in density.

As for the grain size, it can be expressed by the following equation [29]:

$$d^2 - d_o^2 = ke^{-Q/RT}t \tag{4}$$

where d and d_0 are the grain size after and before sintering, T is the sintering temperature, t is the holding time, Q is the activation energy, k and R are constants. According to this model, with higher calcination temperature at the same holding time, crystal boundaries migrate more quickly. The presented results show that both the grain size and the relative density increase with the increase of sintering temperature.

Analysis on degradation behavior of scaffold

Weight Loss of Scaffolds

Figure 5 shows the effects of sintering temperature on the SCPP degradability after soaking in TRIS buffer solution for 45 days. The weight loss of the samples showed a steady increase with the increase of the immersion period. Scaffolds synthesized at different sintering temperatures showed different degradation rate. SCPP900 exhibited the highest degradation rate having weight loss 11.2 % over 45 days of immersion. The degradation rate of SCPP samples for the same holding time increased with the increase of the sintering temperature from 700°C to 900°C.

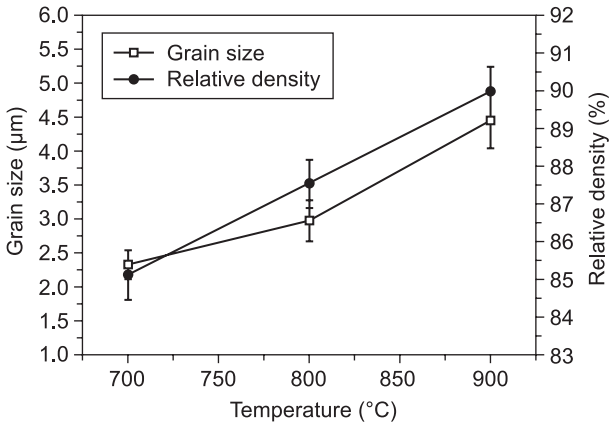

Figure 4. The relative density and grain size of SCPP samples.

Orthophosphate Ion Analysis

CPP is an inorganic polymer with a linear P–O–P backbone which can be cleaved by hydrolysis in aqueous media, with the release of orthophosphate ion as the result [8]. Figure 6 presents the time dependence of PO_4^{3-} concentration in the TRIS solution. It can be seen that all the samples showed a rapid degradation rate within the initial period indicated by an increase of PO_4^{3-} concentration. SCPP900 showed the highest degradation rate having the PO_4^{3-} concentration of 475 mg/l in TRIS buffer solution after 45 days of degradation. The degradation rate of SCPP samples during the same holding time is increasing with the increase in sintering temperature from 700°C to 900°C, These results correspond with the relative weight loss values presented in Figure 5.

Degradability is a concerned property for bone implant materials because it is crucial for bone induction, conduction, metabolism and longevity on implants. The kinetics of biodegradation of the biomaterial should be controlled precisely to give enough time for the cells to lay down their own extracellular matrix and regenegrate the injured bone, and at the same time to ensure that the scaffold does not last longer than needed. Calcium polyphosphate degradation is probably a very complex reaction. According to the theory of Pilliar [8, 9, 23], polyphosphate glasses dissolve in aqueous media in the following two interdependent steps:

1) the amorphous regions are degraded resulting in the high rate of release of degradation products and the rapid loss of strength;

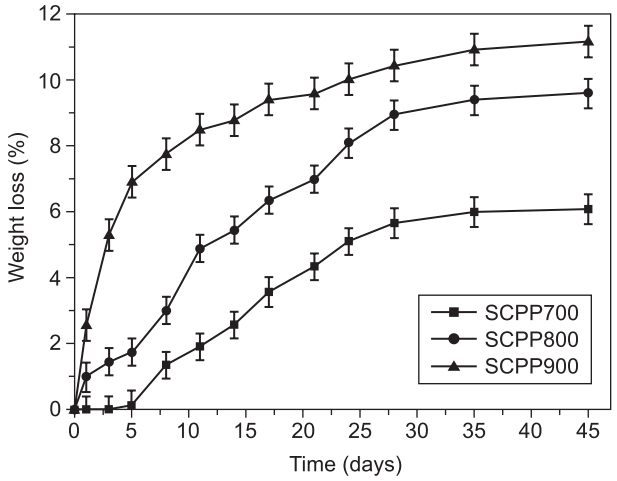

Figure 5. Weight loss of SCPP samples sintered at different temperatures.

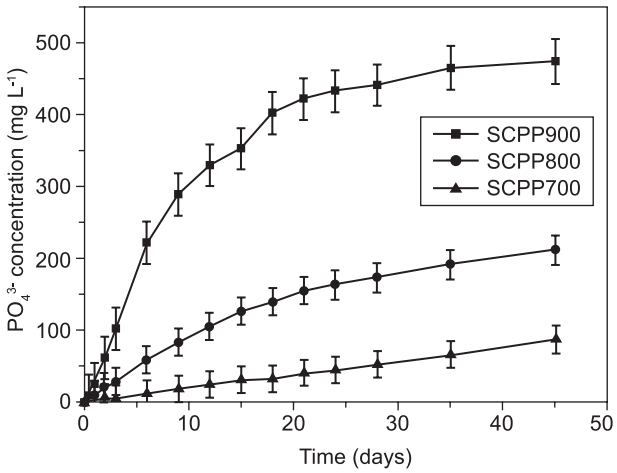

Figure 6. The phosphate ion concentration in the degradation medium for SCPP samples sintered at different temperatures.

2) at later periods of aging the rate of degradation decreases as the degradation of crystallized regions predominates.

Figures 3 and 6 confirmed this assumptions. As showed in Figure 3, SCPP800 and SCPP900 showed clear grain boundaries and the amorphous region were obviously observed in SCPP900. The more grain boundaries and the amorphous region result in the fast degradation of SCPP900. Meanwhile, As shown in Figure 6, all the samples showed a rapid loss of PO_4^{3-} concentration within the initial period of immersion (1st step) followed by a slower loss ratio (2^{nd} step).

Scanning electron microscope analysis

Figure 7 presents the surfaces of SCPP after 45 days degradation. The mineral deposits on the surface could be observed, especially on the surface of SCPP900. The reason is higher degradability of SCPP900 leading to the oversaturation of the solution with PO_4^{3-} and Ca^{2+} and subsequent precipitation on the sample surface.

CONCLUSIONS

In this paper, calcium polyphosphate based bioceramic doping with 1 % Sr^{2+} was prepared at different sintering temperatures. Microstructure and degradability were characterized to investigate the effects of sintering temperature on the performance of SCPP. The results indicated that doped strontium ion did not significantly influence the crystal structure of CPP. The relative density and grain size of SCPP increased with the increase of sintering temperature. The degradation rate of SCPP is also higher, when the sintering temperature increased from 700°C to 900°C. By controlling the sintering temperature, we can obtain SCPP with different microstructures and properties. These findings may provide an approach to study and achieve controllable degradation of SCPP, and explore more biomedical applications.

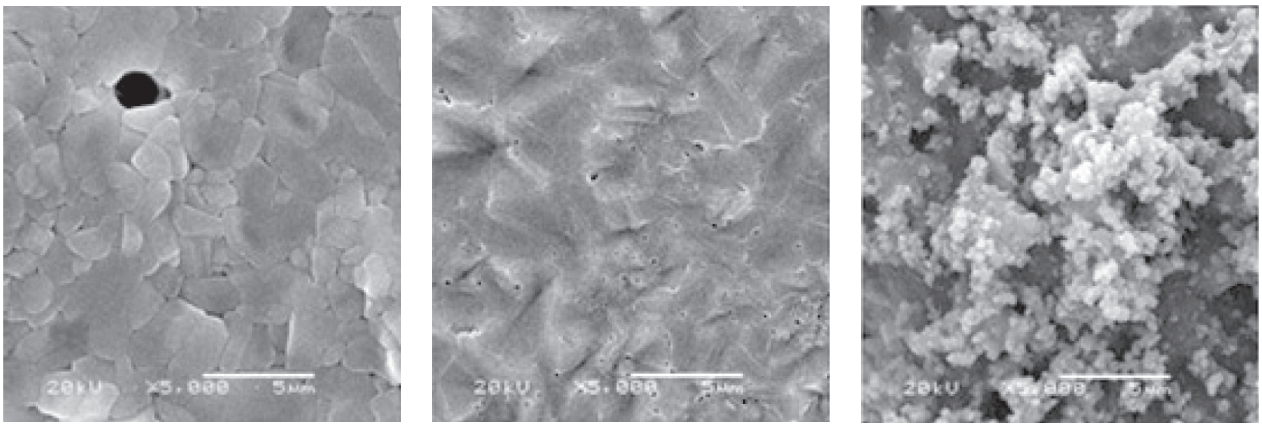

a) b) c)

Figure 7. SEM pictures of SCPP after degradation: a) SCPP700, b) SCPP800, c) SCPP900.

Acknowledgments

The authors are grateful to the NSFC for providing financial support through project 30870614 and 30870616. The author would also like to thank the professors in the Centre of Analysis and Testing of Sichuan University who provided the SEM and XRD measurements.

References

1. Ding Y. L., Chen Y. W., Qin Y. J., Shi G. Q., Yu, X. X., Wan C. X.: Journal of Materials Science-Materials in Medicine *19*, 1291 (2008).
2. Chen F. P., Wang K., Liu C. S.: Applied Surface Science *255*, 270 (2008).
3. Chen F. P., Wang K., Liu C. S., Li W. X.: Chinese Journal of Inorganic Chemistry *24*, 88 (2008).
4. Park E. K.; Lee Y. E., Choi J. Y., Oh S. H., Shin H. I., Kim K. H.: Kim S. Y., Kim S.: Biomaterials *25*, 3403 (2004).
5. Yang S. M., Kim S. Y., Lee S. J., Lee Y. K., Lee Y. M., Ku Y., Chung C. P., Han S. B., Rhyu I. C.: Key Engineering Materials *254*, 245 (2004).
6. Dias A. G., Lopes M. A., Gibson I. R., Santos, J. D.: Journal of Non-Crystalline Solids *330*, 81 (2003).
7. Gomez F., Vast P., Llewellyn P., Rouquerol F.: Journal of Non-Crystalline Solids *222*, 415 (1997).
8. Pilliar R. M., Filiaggi M. J., Wells J. D., Grynpas M. D., Kandel R. A.: Biomaterials *22*, 963 (2001)
9. Grynpas M. D., Pilliar R. M., Kandel R. A., Renlund R., Filiaggi M., Dumitriu M.: Biomaterials *23*, 2063 (2002).
10. El Sayegh T. Y., Pilliar R. M., McCulloch C. A. G.: Journal of Biomedical Materials Research *61*, 482 (2002).
11. Waldman S. D., Grynpas M. D., Pilliar R. M., Kandel R. A.: Journal of Biomedical Materials Research *62*, 323 (2002).
12. Lee Y. M., Seol Y. J., Lim Y. T., Kim S., Han S. B., Rhyu I. C., Baek S. H., Heo S. J., Choi J. Y., Klokkevold P. R., Chung, C. P.: Journal of Biomedical Materials Research *54*, 216 (2001).
13. Qiu K., Wan C. X., Chen X., Zhang Q., Su H. F.: Key Engineering Materials *288*, 553 (2005).
14. Senkoylu A., Yilmaz A., Ergun M. A., Ilhan M. N., Simsek A., Altun N., Bolukbasi S., Menevse S.: Biochemical Genetics *46*, 197 (2008).
15. Canalis E., Hott M., Deloffre P., Tsouderos Y., Marie P.: Bone *18*, 517 (1996).
16. Buehler J., Chappuis P., Saffar J. L., Tsouderos Y., Vignery A.: Bone *29*, 176 (2001).
17. Hott M.. Deloffre P.. Tsouderos Y.. Marie, P.: Bone *33*, 115 (2003).
18. Qiu K., Zhao X. J., Wan C. X., Zhao C. S., Chen Y. W.: Biomaterials *27*, 1277 (2006).
19. Tian M., Chen F., Song W., Song Y. C., Chen Y. W., Wan C. X., Yu X. X., Zhang X. H.: Journal of Materials Science-Materials in Medicine *20*, 1505 (2009).
20. Fiske C. H., Subbarow Y. C. H., Fiske, Subbarow Y.: Journal of Biological Chemistry *66*, 375 (1925)
21. Pauling L.: *The nature of the chemical bond*, p. 335, , 2nd ed., Cornell University, New York 1945.
22 Zhou L.: *Tutorial of physical chemistry*. Beijin, 1st Edition; Science publishing company, Dec.133 (2002). (In Chinese)
23. Porter N. L., Pilliar R. M., Grynpas M. D.: Journal of Biomedical Materials Research *56*, 504 (2001).
24. McIntosh A. O., Jablonski W. L.: Analytical Chemistry *28*, 1424 (2002).
25. Wang K., Chen F. P., Liu C. S., Russel C.: Materials Science & Engineering C-Biomimetic and Supramolecular Systems *28*, 1572 (2008).
26. Guo L. H., Li H., Gao X. H.: Journal of Material Science *39*, 7041 (2004).
27. Weil M., Puchberger M., der Gunne J. S. A.: Weber, Chemistry of Materials *19*, 5067 (2007).
28. Jackson L. E., Kariuki B. M., Smith M. E., Barralet J. E., Wright A.: Chemistry of Materials *17*, 4642 (2005).
29. Pan J. S., Tong J. M., Tian M. B.: *Fundament of Material and Science*, Tsinghua University Press, Beijing 1998. (In Chinese).